ELSEVIER

Journal of Food Engineering **34** (1997) 63–75

Printed in Great Britain
PII: S0260-8774(97)00067-8 0260-8774/98 $19.00+0.00

Numerical Modeling of High Pressure Thawing: Application to Water Thawing

Jean-Marc Chourot*, Lionel Boillereaux, Michel Havet & Alain Le Bail

ENITIAA GPA, Chemin de la Géraudière, BP 82225, 44322, Nantes Cedex 3, France

(Received 11 October 1996; accepted 24 July 1997)

ABSTRACT

A finite difference scheme model which performs both atmospheric and high pressure thawing simulation is presented. The comparison between numerical simulation and experimental data shows a good level of agreement. This model has been used to predict the performance of the thawing process under a wide range of operation conditions. It clearly shows that high pressure thawing reduces the thawing time. © 1998 Elsevier Science Limited. All rights reserved

NOMENCLATURE

$c_{(T)}$	Specific apparent heat (J kg^{-1} K^{-1})
$\tilde{c}_{(T)}$	Volumic apparent heat (J m^{-3} K^{-1})
d	Diameter of the cylinder (m)
$k_{(T)}$, k	Thermal conductivity (W m^{-1} K^{-1})
l	Length of the cylinder (m)
r	Radius (m)
t	Time (s)
F_0	Normalization constant: $\tau k_M/(\rho c_M R^2)$
I	Number of nodes at the radius R
J	Optimization quadratic criterion
L	Latent heat (J kg^{-1})
M	Constant $= \Delta t/\Delta r^2$
P	Pressure (Pa)
R	External radius (m)
T	Temperature (°C)

*To whom all correspondence should be addressed.

U	Overall heat transfer coefficient ($W\ m^{-2}\ K^{-1}$)
Gr_d	Grashof number calculated with $d = 2(R_{vi} - R_{ce})$ (adimensional)
Nu	Nusselt number (adimensional)
Pr	Prandtl number (adimensional)

Greek letters

ρ	Density ($kg\ m^{-3}$)
τ	Maximum simulation time (s)

Subscripts

0	Initial (about temperature)
c	Of copper
ce	Of the external copper cylinder
e	Equivalent
ex	External
f	Of thawing
s	Of steel
M, max	Maximum
min	Minimum
ve	Of the vessel (external)
vi	Of the vessel (internal)
w	Of water

Superscripts

*	Normalized form
n	Time step

INTRODUCTION

High pressure thawing has recently been presented as an alternative to the classical thawing processes, such as air or immersion thawing. Numerous authors explored the potential applications of this process in food technology (Kalichevsky *et al.*, 1995). They reported that high pressure thawing improves food quality and reduces thawing time. Takai *et al.* (1991) studied fish thawing, and Deuchi and Hayashi (1991) tested the behavior of some model substances and beef. Both studies showed a reduction of drip loss.

Even though various numerical models have been developed to predict the thawing times under atmospheric pressure, no data are available for high pressure thawing. Moreover, these models must be suited to high pressure and apply the changes in the thermophysical properties of the foodstuff compounds with the pressure.

The aim of this work is to propose a numerical model describing the kinetics of thawing under both atmospheric and high pressure. To attempt this goal, the model has been designed considering changes in the thermophysical properties with pressure. This numerical model is based on a Crank–Nicolson finite difference scheme (Crank & Nicolson, 1947) applied to an infinite cylinder. This scheme has been chosen for its numerical robustness. The results of the numerical simulations are

validated by the experimental data obtained during the thawing of cylindrical samples made of pure water under atmospheric and high pressures.

MATHEMATICAL MODEL

The heat transfer equation applied to an infinite cylinder is formulated mathematically as follows:

$$\frac{1}{r}\frac{\partial}{\partial r}\left(rk_{(T)}\frac{\partial T}{\partial r}\right)=\rho c_{(T)}\frac{\partial T}{\partial t} \tag{1}$$

To solve eqn (1), the following boundary conditions are considered:

$$r=0,\ \forall t,4k_{(T)}\frac{\partial T}{\partial r}=0$$

$$r=R,\ \forall t,4k_{(T)}\frac{\partial T}{\partial r}=U_{P,T}(T_{(R,t)}-T_{ex}) \tag{2}$$

$$t=0,\ \forall r,4T_{(r,0)}=T_0$$

Many different models are available in the literature to solve the equations describing the thawing or the freezing processes (Crowley, 1978; Mannapperuma & Singh, 1988). Among them, we have chosen the apparent specific heat described by Cleland and Earle (1977) which can be used either as a model substance, like the water in this paper, or with a real food. It is assumed that the density is constant and independent of time. A fixed mesh (Fig. 1) is used in the simulations.

The Crank–Nicolson development of the heat transfer equation (eqn (1)) gives the following matrix main diagonal written with normalized variables:

$$T_{i+1}^{*n+1}\left[\frac{iMF_0}{2(2i-1)}k_{i+1/2}\right]+T_i^{*n+1}\left[\frac{-iMF_0}{2(2i-1)}k_{i+1/2}-\frac{(i-1)MF_0}{2(2i-1)}k_{i-1/2}-\tilde{c}_{(T)}\right]$$

$$+T_{i-1}^{*n+1}\left[\frac{(i-1)MF_0}{2(2i-1)}k_{i-1/2}\right]$$

$$= \tag{3}$$

$$T_{i+1}^{*n}\left[\frac{-iMF_0}{2(2i-1)}k_{i+1/2}\right]+T_i^{*n}\left[\frac{iMF_0}{2(2i-1)}k_{i+1/2}+\frac{(i-1)MF_0}{2(2i-1)}k_{i-1/2}-\tilde{c}_{(T)}\right]$$

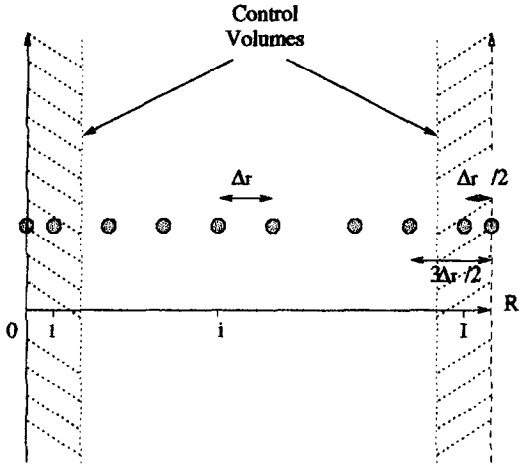

Fig. 1. Space mesh.

$$+T_{i-1}^{*n}\left[-\frac{(i-1)MF_0}{2(2i-1)}k_{i-1/2}\right]$$

with $T-T_{\min}=(T_{\max}-T_{\min})T^*$.

All parameters needed to solve the numerical system are expressed as functions of pressure level and temperature. Also, the phase change temperature and the latent heat L follow the regression equations proposed in Table 1. according to the Bridgman data (Bridgman, 1911). The apparent specific heat is modeled by a triangular function (Fig. 2). The temperature span ΔT_f for the phase change domain is adjusted at 1 K as in Fig. 2. The surface of the apparent specific heat peak represents the latent heat $L(T,P)$ and is adjusted at each time step in order to fit the value of $L(T,P)$ proposed by Bridgman (1911). The maximum temperature of the peak is adjusted with regard to the relation between the phase change temperature and the pressure proposed by Bridgman (1911). Outside the phase change, the data for the specific heat $c_{(T)}$ of water and of ice proposed by Minassian *et al.* (1981) are used.

The transition between the thermal conductivity of the solid and that of the liquid during the phase change is modeled using a parallel conduction model. The ratio

TABLE 1
Regression Equations of Thermophysical Properties of Water

L (J kg^{-1})	$333\,549{\cdot}295-399{\cdot}369P-0{\cdot}388P^2$
T_f (°C)	$-0{\cdot}072\,192P-0{\cdot}000\,155P^2$

Pressure P/MPa.

between water and ice is supposed to be a linear function of the temperature over the phase change gap. In the absence of data, the thermal conductivity of ice at atmospheric pressure is used and assumed to be constant. For the same reason, the thermal conductivity of liquid water at 50 MPa is used above this pressure.

The overall heat transfer coefficient $U_{(P,T)}$ results from the conductive heat transfer in the internal steel wall of the vessel, from the convective heat transfer in the annular gap between the sample and the water-filled vessel, and from the conductive heat transfer in the copper wall of the sample (eqn (6)). The natural convection in an annular gap can be described by the correlation in eqn (4).

$$\mathrm{Nu} = \alpha(\mathrm{Pr}\ \mathrm{Gr})^{\beta}\left(\frac{l}{d}\right)^{\gamma} \tag{4}$$

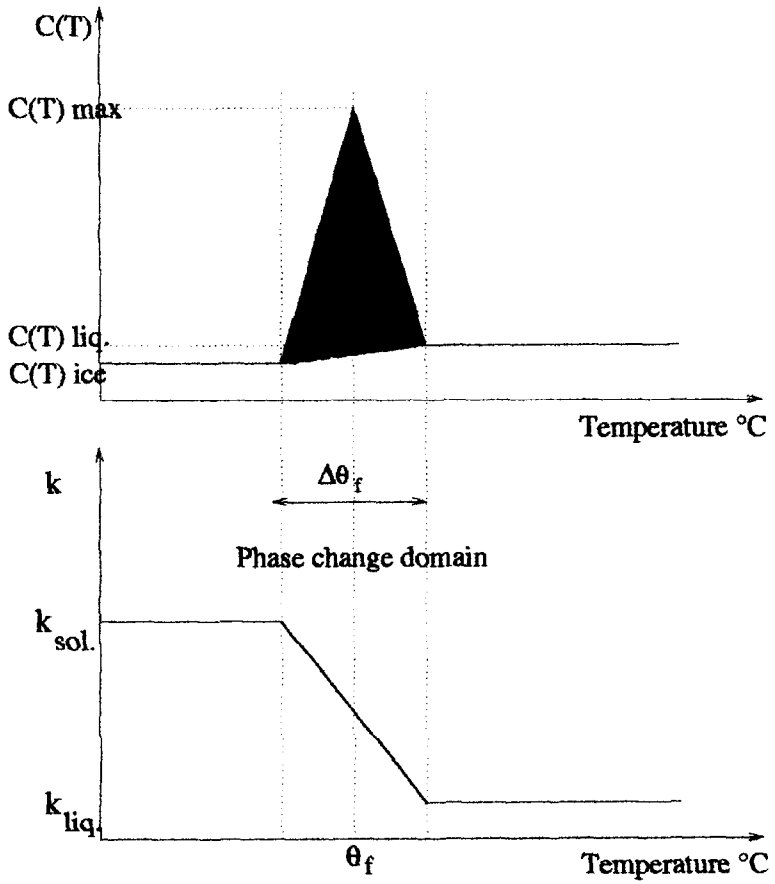

Fig. 2. Heat capacity and thermal conductivity evolutions.

Amongst the available relations cited by Giblin (1974) for an annular gap, the relation proposed by Sheriff (1966) was chosen first. As the coefficients depend on the physical properties of the fluid, the triplets (α, β, γ) have to be optimized (see Section 4.2.).

In the Sheriff relation, the Nusselt number represents the ratio between the effective thermal conductivity k_e of the annular gap and the thermal conductivity of the fluid, as shown in eqn (5).

$$\mathrm{Nu} = \frac{k_e}{k_w} = 0{\cdot}250(\mathrm{Gr}_d\,\mathrm{Pr})^{0{\cdot}30}\left(\frac{l}{d}\right)^{-0{\cdot}25} \tag{5}$$

The thermophysical properties of water proposed by Alexander (1981) and Tanishita *et al.* (1971) are retained to calculate the Grashof and the Prandtl numbers. The effective thermal conductivity of the annular gap k_e is then used for the computation of the overall heat transfer coefficient described in eqn (6).

$$U_{(P,T)} = \frac{1}{2\pi R_{\max}\left[\ln\left(\frac{R_{ve}}{R_{vi}}\right)\frac{1}{2\pi k_s} + \ln\left(\frac{R_{vi}}{R_{ce}}\right)\frac{1}{2\pi k_e} + \ln\left(\frac{R_{ce}}{R_{\max}}\right)\frac{1}{2\pi k_c}\right]} \tag{6}$$

EXPERIMENTAL

High pressure experiments were performed in a high pressure vessel (internal diameter 120 mm, height 300 mm; Fig. 3).

The ambient temperature in the vessel was maintained by an external circulating bath at 10°C during the high pressure assay and at 19°C under atmospheric pressure. The samples were of cylindrical geometry (50 mm internal diameter for high pressure, and 40 mm diameter for atmospheric conditions) with ratio diameter/length equal to 0·17 and 0·14 respectively. They were made of a copper cylinder (50 mm I.D., 1 mm thickness) filled with distilled water and nylon wool (porosity 0·976) to avoid convection in the liquid after thawing. Both ends of the sample were insulated by a 1 cm thickness PVC disk which kept the probes in place. The samples were initially frozen and stored at −78°C.

For pressure resistance reasons, the thermal probes (thermocouples of J type, 1 mm diameter) were previously installed through the obturator. The samples were equipped with three aluminum guides (internal diameter 1 mm, external diameter 2 mm). They were placed resistively at the center, at the half-radius and at the surface of the sample. The installation of the sample consisted of placing the thermocouples in the aluminum guides and then to thread the obturator onto the high pressure vessel. A high pressure pump pressurized the vessel in less than 2 min. Temperatures were collected every 30 s.

RESULTS AND DISCUSSION

Validation

The model is validated in comparing the analytical solution of the heat diffusion equation (Carslaw & Jaeger, 1959) to the model under atmospheric condition and without phase change. When comparing the curves T vs t of two models, a satisfying agreement is obtained (maximum deviation of 1% for heating from 0 to 100°C).

In the case of a phase change, the consistency is tested with regard to the time step and the number of nodes. Figure 4 shows the influence of the parameters on the thawing time in the case of an infinite cylinder of ice (diameter 5 cm). Initial and ambient temperatures were -20°C and 20°C respectively. The model requires a number of nodes greater than 80 and a time step lower than 5 s to be insensitive to those parameters. The values of the time step and of the number of nodes which have been kept to achieve the computation in the sequel were respectively equal to 1 s and 120.

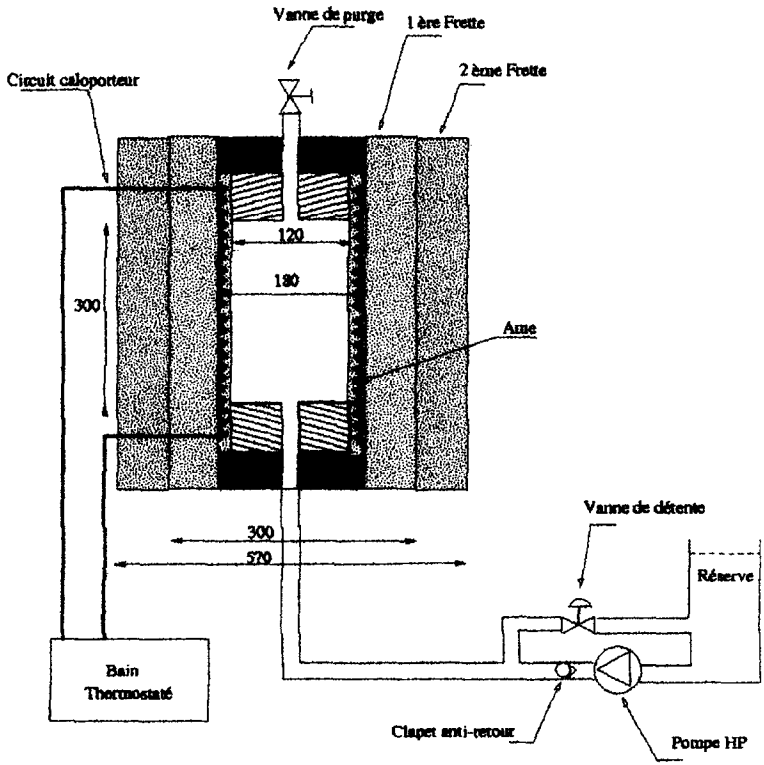

Fig. 3. Experimental pilot.

Optimization of the convective heat transfer coefficient

The numerical coefficients α, β, γ of the expression proposed by Sheriff (eqn (5)) for eqn (4) have been optimized in comparing the experimental and the numerical results for the set of experiments. A Quasi-Newton method has been used (Davidon–Fletcher–Powell method) (Dennis & More, 1977; Minoux, 1983) for the estimation of the Hessian matrix.

This method consists of minimizing a criterion which, in this case, is

$$J = \frac{1}{N} \sum_{i=1}^{N} \{[T_{r=0}(i) - \hat{T}_{r=0}(i)]^2 + [T_{r=R/2}(i) - \hat{T}_{r=R/2}(i)]^2 + [T_{r=R}(i) - \hat{T}_{r=R}(i)]^2\} \quad (7)$$

where N is the number of points, $T_{r=x}$ the experimental temperatures at the radius x and $\hat{T}_{r=x}$ the estimated temperature given by the model at the radius x. As the sample geometry is fixed, the aspect ratio is a constant, and thus the constant α was fixed at 0·25. Only, β and γ have been optimized. The many different runs of the optimization algorithm showed that the procedure allowed one to reach the absolute minimum. The results confirmed that Sherrif values were the optimal ones in our case.

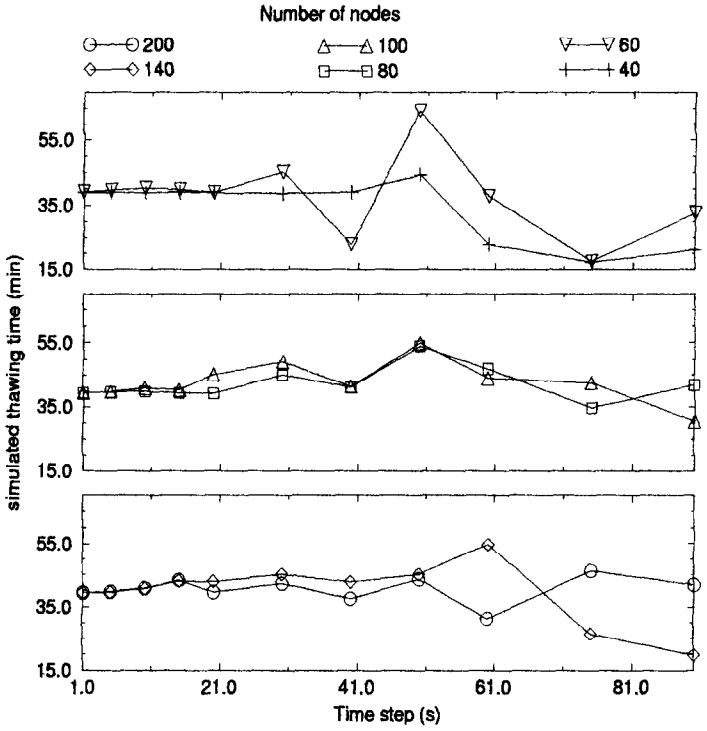

Fig. 4. Consistency of the model versus time step and space mesh through predicted thawing time.

Comparison with experimental results

The model can be compared with experiments under atmospheric pressure (Fig. 5) and under high pressure (Fig. 6). In both cases, the calculated and the experimental thawing times are in accordance. The experimental temperature changes are well fitted by the model under atmospheric as well under high pressure conditions, in spite of a difference between the very beginning of the high pressure experimental and numerical curves. This difference can be explained by two main reasons. First, because of the high pressure technology, an averaged time of 3 min is wasted during the preparatory phase (probes guiding, closing the vessel and pressurizing). During that time, the thermal probes cannot be plugged to the data acquisition system, but the thawing of the sample starts. Thus, the lack of experimental data during the preparatory phase introduces an inaccuracy in the initial temperature distribution in the sample. These transient phenomena cannot be taken into account in the model. Second, during the pressurization phase, two phenomena might occur. On the one hand, if the temperature of the thawed outer surface reaches values close to 4°C, an increase of the pressure cools down the liquid. This first phenomenon is related to the change of the slope of the thermal expansion coefficient (Minassian *et al.*, 1981). On the other hand, when the surface temperature reaches the phase change temperature corresponding to the pressure in the vessel, the surface temperature slides on the melting curve while the pressure increases. Indeed, the phase change energy cannot be balanced by the incoming heat flux. For those reasons, the comparison with the model must not be taken into account until the nominal pressure is reached.

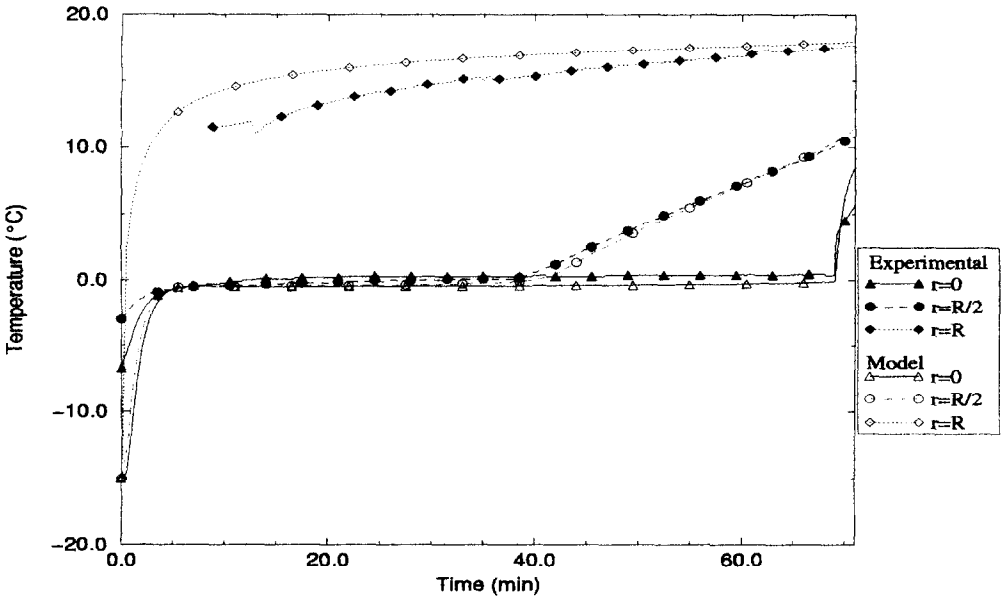

Fig. 5. Experimental data versus model under atmospheric pressure ($R = 4$ cm).

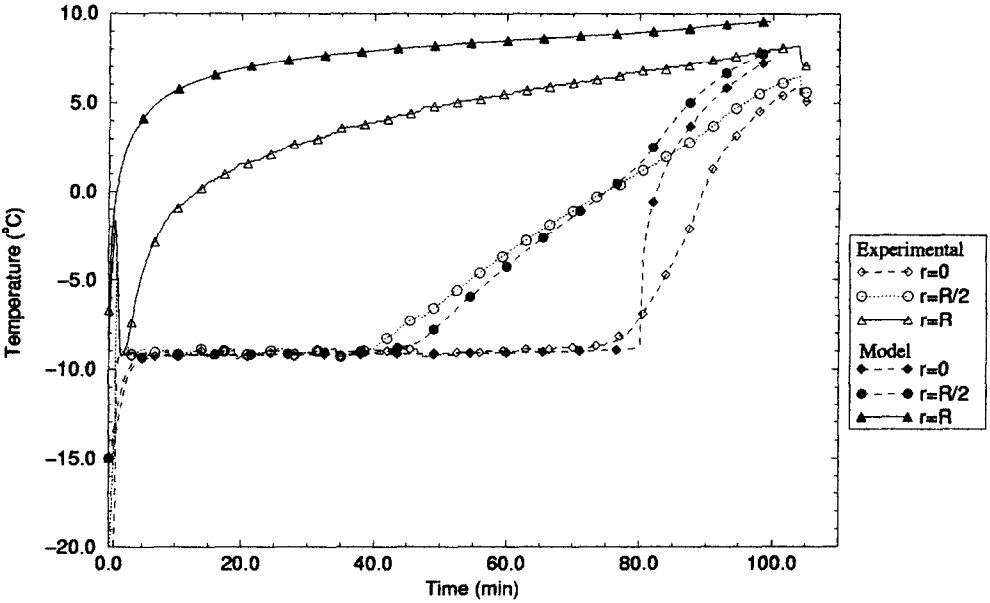

Fig. 6. Experimental data versus model ($R = 5$ cm, $T_0 = 0$°C, $T_{ex} = 10$°C).

At the surface, the difference between calculated and experimental temperatures can be explained by the fact that the guides enclosing the thermal probes are too large to consider that the measured temperature is exactly that of the surface. Therefore, the surface data collected must be considered as the mean value of the guide section.

At the center, the liquid phase part of the curves differs slightly under high pressure thawing. The time necessary to reach 0°C is underestimated by 7·8%. Nevertheless, the phase change at the center and the experimental data at $r = R/2$ are well described by the model. At the end of the experiments, the decompression yields a cooling of the pressurization media and of the sample. This is not yet taken into account in the model but is planned to be coded.

Explanatory tool

The model has been used as a tool to improve the understanding of heat transfer phenomena during high pressure thawing. The contribution of two parameters in the decrease of the thawing time is presented: (i) the influence of the decrease of the latent heat; (ii) the influence of the temperature gap between T_f and T_{ex}. Then, the influence of the sample size is presented.

To avoid the influence of a different temperature gradient during the process, constant temperature gaps have been imposed between the fusion temperature T_f ($-14{\cdot}3$°C at 150 MPa and $-8{\cdot}8$°C at 100 MPa) and the external temperature T_{ex}, and between T_{ex} and the initial temperature of the sample T_0. The curves are plotted in Fig. 7. The effect of the decrease of L and of the specific heat of the

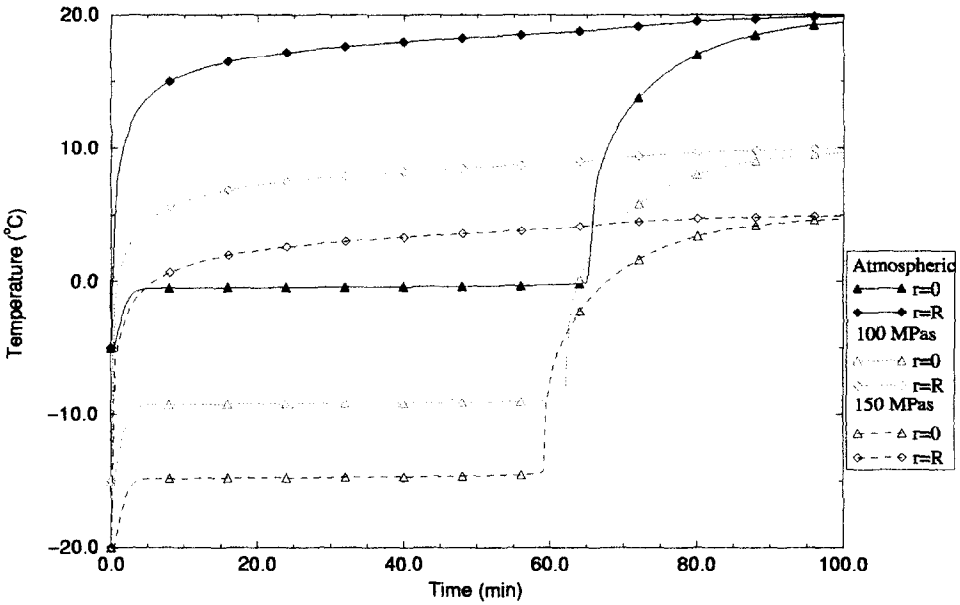

Fig. 7. Influence of the evolution of thermophysical properties on thawing time ($R = 5$ cm, $T_0 = T_f - 5$°C, $T_{ex} - T_0 = 25$°C, $I = 120$, $\Delta t = 1$ s, $P = 0.1$, $P = 150$ and $P = 100$ MPa).

liquid consists in a reduction of almost 10% in the thawing time between 0.1 MPa and 150 MPa.

The difference between the freezing point of the material and the external media temperature is the main factor which most affects the reduction in the thawing time (Fig. 8). The thawing time is reduced by a factor of three between atmospheric conditions and 150 MPa. This gap allows a larger incoming heat flux and then, associated with the decrease of L, reduces the thawing time.

The simulations (Fig. 9) on various radius and pressure levels show that the greater the sample volume is, the more saved time is important. Nevertheless, the ratios of the thawing times between two radii at a given pressure level are maintained over the pressure span. The time evolution with the pressure level follows a quadratic regression.

CONCLUSION

A numerical model based on a Crank–Nicolson scheme is available for numerical simulation of high pressure thawing. This model, developed for a cylinder geometry, takes into account the evolution of thermophysical properties with the pressure. Numerical results fit well the experimental data obtained under atmospheric pressure and high pressure and with respect to the thawing time of the sample. Used as a simulation tool, the model shows that, under high pressure, the thawing can take place in a media close to 0°C without any loss of time if compared with the

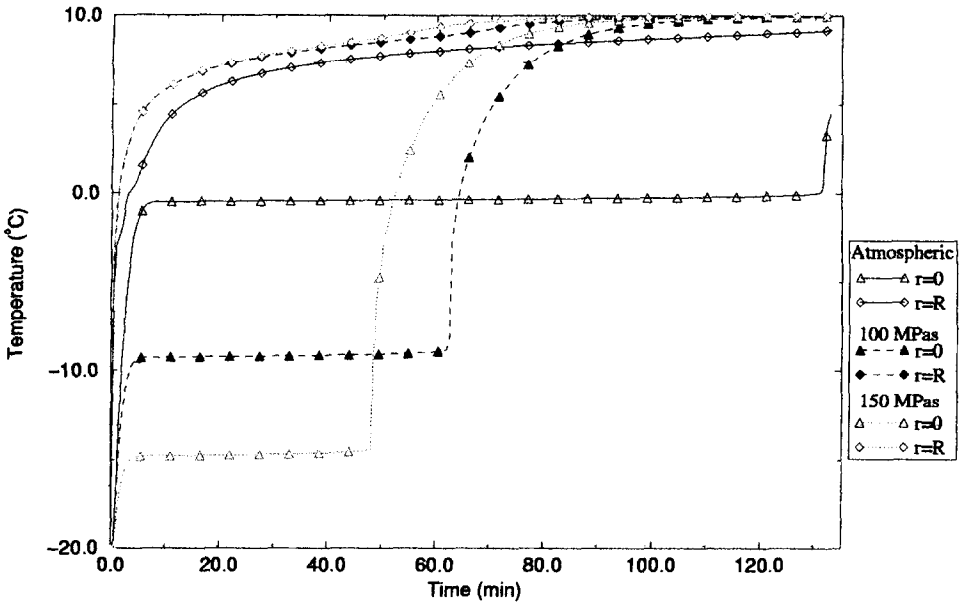

Fig. 8. Atmospheric model data versus high pressure model results at $T_{ex} = 10°C$ ($R = 5$ cm, $T_0 = -20°C$, $I = 120$, $\Delta t = 1$ s, $P = 0.1$).

atmospheric conditions. This could be used for an extremely thermo-sensible product. As many different compounds are found in real foodstuffs, this model will change in accepting real foodstuffs experimental thermophysical properties when available. It will soon take into account the pressure slope with time and the relative heating or cooling phenomenon.

REFERENCES

Alexander, D. M. (1981). The viscosity of liquids at high pressure. *Australian Journal of Chemistry* **34**, 1567–1571.

Bridgman, P. W. (1911). Water in the liquid and five solid forms under pressure. *Proceedings of the American Academy of Arts and Sciences* **47**, 441–558.

Carslaw, H. S. & Jaeger, J. C. (1959). *Conduction of Heat in Solids*. Clarendon Press.

Cleland, A. C. & Earle, R. L. (1977). The third kind of boundary condition in numerical freezing calculations. *International Journal of Heat and Mass Transfer* **20**, 1029–1034.

Crank, J. & Nicolson, P. (1947). A practical method for numerical evaluation of solutions of partial differential equation of the heat-conduction type. *Proceedings of the Cambridge Philosophical Society* **43**, 50–67.

Crowley, A. B. (1978). Numerical solution of Stephan problems. *International Journal of Heat and Mass Transfer* **21**, 215–219.

Dennis, J. E. & More, J. J. (1977). Quasi-Newton methods, motivation and theory. *S.I.A.M. Review* **19**(1), 46–89.

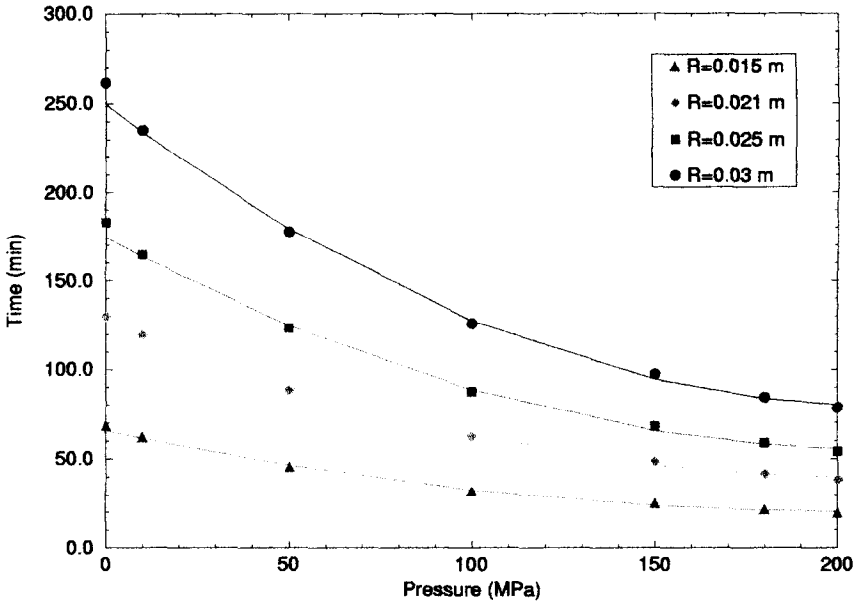

Fig. 9. Influence of pressure level on thawing dwell time for various cylinder radii ($T_0 = -20°C$, $T_{ex} = 10°C$, $I = 120$, $\Delta t = 1$ s).

Deuchi, T. & Hayashi, R. (1991). Pressure application to thawing of freezed foods and to food preservation under subzero-temperature. In *High Pressure Science for Food*, ed. R. Hayashi, pp. 101–110. John Libbey Eurotext.

Giblin, R. (1974). *Transmission de la Chaleur par Convection Naturelle*. Eyrolles.

Kalichevsky, M. T., Knorr, D. & Lillford, P. J. (1995). Potential food applications of high-pressure effects on ice–water transitions. *Trends in Food Science and Technology* **6**, 253–259.

Mannapperuma, J. D. & Singh, R. P. (1988). Prediction of freezing and thawing times of foods using a numerical method based on enthalpy formulation. *Journal of Food Science* **53**, 2 626–630.

Minassian, L. T., Pruzan, P. & Soulard, A. (1981). Thermodynamic properties of water under pressure up to 5 kbar and between 28 and 120°C. Estimation in the supercooled region down to −40°C. *Journal of Chemical Physics* **75**(6), 3064–3072.

Minoux, M. (1983). *Programmation Mathématique, Théorie et Algorithmes*, Vol. 1. Dunod.

Sheriff, N. (1966). Experimental investigation of the natural convection in single and multiple vertical annuli with high pressure carbon dioxide. In *3rd International Heat Transfer Conference*, Vol. 2. AICHE.

Takai, R., Kozhima, T. & Suzuki, T. (1991). Low temperature thawing by using high pressure, *Les Actes du XVIIe Congrès International du Froid*, Vol. 4. pp. 1951–1955.

Tanishita, I., Nagashima, A. & Murai, Y. (1971). Correlation of viscosity, thermal conductivity, and Prandtl number for water and steam as a function of temperature and pressure. *Bulletin of the JSME* **14**(77), 1187–1197. Institut International du froid.